

# Solvent-enabled photodissociation of $\text{CO}_2^-$ in water clusters

Terefe Habteyes, Luis Velarde, Andrei Sanov \*

*Department of Chemistry, University of Arizona, 1306 E. University Boulevard, Tucson, AZ 85721-0041, USA*

Received 20 February 2006; in final form 13 April 2006

Available online 28 April 2006

## Abstract

The photofragmentation of  $\text{CO}_2^-(\text{H}_2\text{O})_m$ ,  $m = 3\text{--}20$  at 355 nm yields two types of anionic products:  $\text{O}^-(\text{H}_2\text{O})_{m-k}$ ,  $1 \leq k \leq 3$ , and  $\text{CO}_2^-(\text{H}_2\text{O})_{m-k}$ ,  $4 \leq k \leq 9$ , depending on the parent cluster size. The  $\text{O}^-(\text{H}_2\text{O})_{m-k}$  fragments, attributed to the dissociation of hydrated  $\text{CO}_2^-$ , are dominant for  $m = 3\text{--}7$ , while the water-evaporation products,  $\text{CO}_2^-(\text{H}_2\text{O})_{m-k}$ , take precedence for  $m = 8\text{--}20$ . The dissociation of  $\text{CO}_2^-$  is proposed to proceed via a hydration-stabilized excited state, originating from a low-lying  $\text{CO}_2^-$  resonance. In the evaporation channel, the suggested routes include cluster predissociation,  $\text{CO}_2^-$  photodissociation/recombination, and charge transfer to solvent.  
© 2006 Elsevier B.V. All rights reserved.

## 1. Introduction

The outcomes of chemical reactions are affected by interactions with the environment. This paper spotlights solvent-enabled chemistry in heterogeneous cluster anions, focusing on reaction pathways made possible by the presence of the solvent. Specifically, we examine the photochemistry of  $\text{CO}_2^-$  [1–3] trapped in the network of up to 20 water molecules and observe a solvation-induced shift from electron photodetachment towards the breaking of covalent bonds.

Due to the relatively low electron detachment energies, many excited electronic states of negative ions exist as short-lived resonances embedded in the free-electron continuum. These states play pivotal roles in interactions of low-energy electrons and neutral molecules, as well as the dissociation and electron detachment dynamics of negative ions [4]. The lifetimes of anionic resonances can be effectively tuned using stepwise solvation in cluster-ion environments. With sufficient stabilization, the resonances move from the detachment continuum into the range of stable (electron-bound) states, opening new, solvent-enabled pathways for anionic reactions.

Metastable anions of  $\text{CO}_2$  in the gas phase were first observed by Cooper and Compton [1,2]. Despite the markedly negative adiabatic electron affinity of  $\text{CO}_2$  ( $-0.60 \pm 0.2$  eV [3]),  $\text{CO}_2^-$  has a long autodetachment lifetime of 60–90  $\mu\text{s}$  [1,3], attributed to the geometry difference between the anion and neutral equilibria. Namely, at the bent equilibrium geometry of  $\text{CO}_2^-$ , the anion energy is lower than that of the corresponding neutral [5,6]. The metastable anions can be further stabilized by solvation; for instance, Klots reported the formation of  $(\text{CO}_2)_n^-(\text{H}_2\text{O})_m$ , which did not exhibit autodetachment even for  $n = m = 1$  [7]. Both the experiment and theory show that the excess electron in  $\text{CO}_2^-(\text{H}_2\text{O})_m$  clusters is localized on  $\text{CO}_2$  [8].

The work reported here builds on our group's earlier photoelectron imaging study of the  $(\text{CO}_2)_n^-(\text{H}_2\text{O})_m$ ,  $n = 1\text{--}12$ ,  $m = 0\text{--}6$  cluster anions [8,9]. The experiments indicated the dominance of photoinduced autodetachment over direct photodetachment in the presence of four or more water molecules. Disappointingly, however, photoelectron imaging revealed little about the nature of the excited autodetaching states. To complete the picture, one must elucidate the decay of the excited states via different competing pathways, including the electron detachment and anionic fragmentation of the cluster. In this work, we use tandem time-of-flight mass-spectroscopy to examine 355 nm fragmentation of size-selected  $\text{CO}_2^-(\text{H}_2\text{O})_m$ ,

\* Corresponding author. Fax: +1 520 621 8407.

E-mail address: [sanov@u.arizona.edu](mailto:sanov@u.arizona.edu) (A. Sanov).

$m = 3$ –20 cluster ions. The reported photodissociation of the  $\text{CO}_2^-$  core in these clusters illuminates the role of excited anionic states stabilized by interactions with the water network.

## 2. Experimental apparatus

The experiments were carried out on a new experimental apparatus. Its detailed description is forthcoming, with only the most pertinent features outlined here. As used in this work, the instrument consists of a cluster-ion source and a tandem time-of-flight (TOF) mass-spectrometer, utilizing the ion generation and analysis techniques pioneered by Lineberger and co-workers [10]. The ion source and the primary TOF parts of this new instrument are also similar to our photoelectron imaging machine described elsewhere [11].

The  $\text{CO}_2^-(\text{H}_2\text{O})_m$  cluster anions are prepared by expansion of undried  $\text{CO}_2$  at a stagnation pressure of 2 atm through a pulsed supersonic nozzle (General Valve Series 99, 0.8 mm nozzle diameter) into a vacuum chamber with a base pressure of  $2 \times 10^{-7}$  Torr.  $\text{CO}_2$  tank impurities and trace amounts of water within the gas delivery lines serve as sources of  $\text{H}_2\text{O}$ . A 1 keV electron beam ionizes the supersonic expansion close to the valve orifice. The cluster anions are formed by secondary-electron attachment to neutral clusters [10]. A transverse, pulsed electric field ( $\sim 1$  kV/15 cm) is applied approximately 18 cm downstream from the supersonic valve to extract the ions into the 2.3 m long flight tube of a Wiley–McLaren TOF mass-spectrometer, where they are further accelerated to a beam energy of 3 keV.

After passing through a set of ion optical components [11], the ions are brought to a temporal and spatial focus in the detection region of the instrument (base pressure  $5 \times 10^{-9}$  Torr). They are detected with temporal resolution using an in-line microchannel plate (MCP) detector mounted at the end of the flight-tube. The mass-selected cluster anions of interest are interrogated with a pulsed laser beam. The ionic photofragments are analyzed with a single-field reflectron mass-spectrometer, where the parent and assorted fragment ions are separated according to their mass. The reflectron assembly is tilted by a  $2.5^\circ$  angle with respect to the primary TOF axis, deflecting the reflected ions by  $5^\circ$  relative to the incoming beam. The reflected fragments are detected by an off-axis MCP detector at the spatial focus of the reflectron.

The third harmonic of a Nd:YAG laser (Spectra Physics, model Lab 130-50) gives 355 nm, 15 mJ nanosecond pulses at a repetition rate of 50 Hz. The laser beam is brought to a 5 mm diameter spot size inside the vacuum chamber. The ionic photofragments arising from the mass-selected parent anions are detected and analyzed as described elsewhere [12,13]. The mass-spectra obtained by focusing the reflectron on different fragments arising from the same parent ions are averaged for  $\sim 500$  laser shots. They are then assembled into a combined mass-spectrum

representing all observed fragmentation channels of the parent ion studied.

## 3. Results

A representative  $\text{CO}_2^-(\text{H}_2\text{O})_m$  parent-ion mass-spectrum is shown in Fig. 1. The intensity pattern is reproducible at varying source conditions and consistent with the previous report by Tsukuda et al. [14].

Absorption of visible/UV light by a cluster anion generally leads to electron detachment or photofragmentation. The former process was the focus of our previous work [8], which indicated that due to the rise in the vertical detachment energy of  $\text{CO}_2^-(\text{H}_2\text{O})_m$ , the yield of 400 nm photodetachment decreases with increasing  $m$ , nearly vanishing for  $m > 6$ . In the present work, we observed a sharp increase in the photofragment ion yield relative to the parent depletion signal at 355 nm for the  $\text{CO}_2^-(\text{H}_2\text{O})_m$ ,  $m > 7$  clusters, compared to  $m < 7$ . The photofragmentation is observed as a minor channel in the small-size range, becoming the dominant photodestruction pathway in the larger clusters.

The photofragment ion mass-spectra obtained at 355 nm for mass-selected  $\text{CO}_2^-(\text{H}_2\text{O})_m$ ,  $m = 3$ –20 are shown in Fig. 2. The spectra are normalized to the same maximum intensity, not representative of the corresponding absolute cross-sections. We verified, however, that the integrated peak intensities for selected fragment ions scale linearly with laser power, confirming the one-photon nature of the transitions. No anionic fragmentation of  $\text{CO}_2^-(\text{H}_2\text{O})_m$  was observed at 532 nm.

The 355 nm spectra reveal two types of fragment anions: (1)  $\text{O}^-(\text{H}_2\text{O})_{m-k}$ ,  $1 \leq k \leq 3$ , and (2)  $\text{CO}_2^-(\text{H}_2\text{O})_{m-k}$ ,  $4 \leq k \leq 9$ . No  $(\text{H}_2\text{O})_{m-k}^-$  fragments are observed. The appearance of the  $\text{O}^-(\text{H}_2\text{O})_{m-k}$  fragments implies the dissociation of the  $\text{CO}_2^-$  core of the cluster, followed by the escape of CO and evaporation of  $k\text{H}_2\text{O}$  molecules:

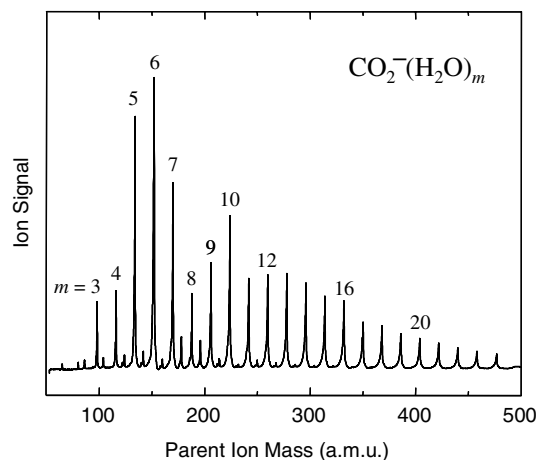
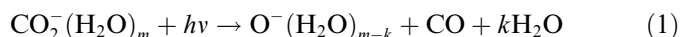


Fig. 1. Mass-spectrum of parent  $\text{CO}_2^-(\text{H}_2\text{O})_m$  cluster anions.

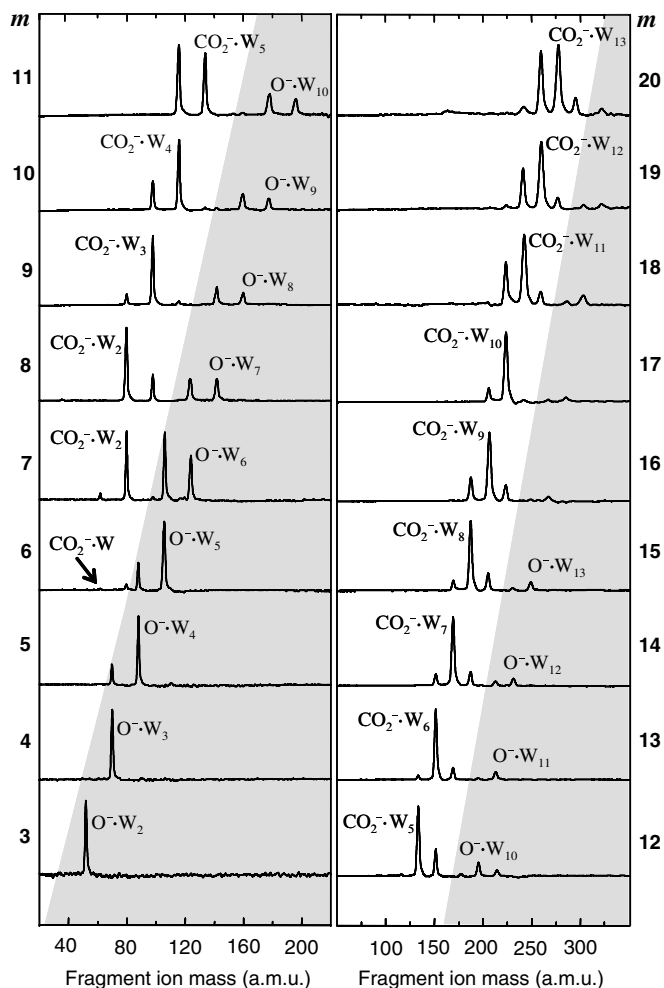
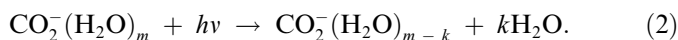


Fig. 2. Photofragment mass-spectra obtained from  $\text{CO}_2^-(\text{H}_2\text{O})_m$ ,  $m = 3$ – $20$  cluster anions at 355 nm. Partial shading is provided for visual separation of the core-dissociation products,  $\text{O}^-(\text{H}_2\text{O})_{m-k}$  (shown against gray background) from the evaporation products,  $\text{CO}_2^-(\text{H}_2\text{O})_{m-k}$  (clear background).  $\text{W} \equiv \text{H}_2\text{O}$ .

We will refer to all pathways defined by Eq. (1) collectively as the core-dissociation channel. The  $\text{CO}_2^-(\text{H}_2\text{O})_{m-k}$  fragments will be described as water-evaporation products, formed via:



As evident from Fig. 2, the  $\text{CO}_2^-(\text{H}_2\text{O})_m$ ,  $m = 3$ – $5$  cluster anions yield only the core-dissociation fragments. As the parent cluster size is increased, the water-evaporation fragments first appear at  $m = 6$ , with the smallest fragment of this type being  $\text{CO}_2^- \cdot \text{H}_2\text{O}$ . With  $m$  increasing further, the evaporation channel gradually takes over to become the dominant pathway for  $m \geq 8$ . The branching between channels (1, 2) is summarized in Fig. 3 as a function of the parent cluster size.

The average loss of water molecules in channels (1) and (2) is  $\langle k \rangle = 1.0$ – $2.5$  and  $4.4$ – $7.5$ , respectively, depending on the parent size. In both channels,  $\langle k \rangle$  increases with  $m$ . Assuming that the  $\text{H}_2\text{O}$  loss in channel (2) accounts for

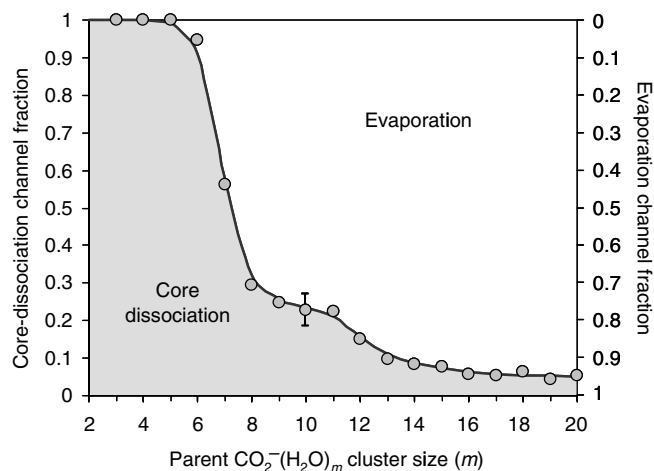


Fig. 3. Branching ratio of the core-dissociation and water-evaporation fragments as a function of the parent cluster size. The solid trend line and shading are added to guide the eye.

the dissipation of all of 355 nm photon energy, the average binding energy of one  $\text{H}_2\text{O}$  to the cluster is estimated as 0.47 eV (in the limit of large  $m$ ).

#### 4. Discussion

The electronic excitation responsible for the observed fragmentation of the  $\text{CO}_2^-(\text{H}_2\text{O})_m$  cluster anions by UV light can either be localized on the  $\text{CO}_2^-$  core of the cluster or involve a charge transfer to solvent (CTTS). Either type of excitation may be followed by anionic fragmentation or autodetachment, provided there is enough energy for the removal of the electron.

The core-dissociation channels (1) definitely involve the excitation of the  $\text{CO}_2^-$  core of the cluster. The water-evaporation pathways, on the other hand are consistent with three distinct mechanisms: (2-i) cluster predissociation via electronic excitation of  $\text{CO}_2^-$  followed by energy transfer to inter-molecular degrees of freedom; (2-ii) photodissociation of  $\text{CO}_2^-$  followed by its recombination or trapping of the CO fragment within the cluster; (2-iii) a CTTS transition followed by the evaporation of several  $\text{H}_2\text{O}$  molecules. Since no  $(\text{H}_2\text{O})_{m-k}^-$  fragments are observed, the possible CTTS process is likely reversed by electron recapture by the  $\text{CO}_2$ .

The decrease in the fraction of core-dissociation fragments with increasing parent cluster size (Fig. 3) is consistent with all of these mechanisms. For example, in (2-iii) the increase in the relative yield of the water-evaporation fragments in larger parent clusters may reflect the closing of the indirect detachment channel. Without autodetachment, the evaporation becomes the main decay mechanism for the CTTS states. The sharp increase in the water-evaporation fraction occurring between  $m = 6$  and  $8$  seen in Fig. 3 coincides with the size range where we expect the autodetachment pathway to close in 355 nm experiments [8].

In summary, the excited states of  $\text{CO}_2^-$  play a defining role in the photofragmentation of the  $\text{CO}_2^-(\text{H}_2\text{O})_m$  cluster anions via channel (1). Their participation is also possible in channel (2). We will now focus on the nature of the relevant states and their dissociation dynamics.

The UV absorption spectrum of  $\text{CO}_2^-$  in a crystalline matrix consists of three bands with maxima at 340, 280 and 250 nm [15], while only a single band peaking at 250 nm was observed in aqueous solution [16]. The 340 nm band, also seen by Hartman and Hisatsune at 365 nm [17], is most relevant to our 355 nm experiments.

From thermochemistry [18], the bond dissociation energy of  $\text{CO}_2^-$  is calculated as  $3.46 \pm 0.20$  eV, not accounting for differential solvation of the parent  $\text{CO}_2^-$  and the fragment  $\text{O}^-$  ions. In  $\text{CO}_2^-(\text{H}_2\text{O})_m$ , the dissociation energy of the  $\text{CO}_2^-$  core is expected to be smaller.

Formation of  $\text{O}^-$  has long been observed by dissociative electron attachment to  $\text{CO}_2$  both in the gas phase [19–21] and in condensed environments [22]. The process is understood in terms of a short-lived anion intermediate that undergoes dissociation into stable  $\text{O}^- + \text{CO}$ . Of special interest to this work is the peak in the  $e^- + \text{CO}_2$  cross-section at 3–4 eV [20,21]. In this range, the attachment occurs via the  ${}^2\Pi_u$  shape resonance, with the electron entering a low lying degenerate  $\pi_u$  orbitals, which arises from an antibonding combination of the 2p orbitals of O, C, and O. The  ${}^2\Pi_u$  resonance peaks at 3.8 eV and has an autodetachment lifetime of only a few femtoseconds (in the gas phase) [20,23]. Its degeneracy is lifted when the molecule bends, splitting the  ${}^2\Pi_u$  state into the  ${}^2A_1$  and  ${}^2B_1$  Renner–Teller components [5]. The corresponding potential energy curves, calculated [24] at the MP2 level with the 6-311G\* basis set, are shown in Fig. 4.

This classic Renner–Teller picture is complicated by the existence of a third low-lying state, described as a virtual  ${}^2\Sigma_g^+$  state [25,26]. In this state, the excess electron occupies a very diffuse, totally symmetric orbital, which can be viewed approximately as a free-electron perturbed by the

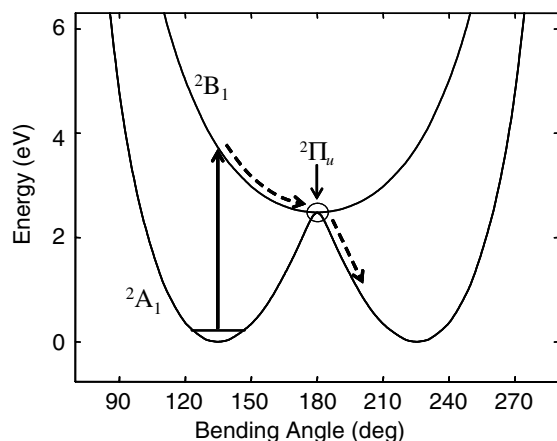


Fig. 4. Bending potential energy curves for the  ${}^2A_1$  and  ${}^2B_1$  electronic states arising from the  ${}^2\Pi_u$  resonance in  $\text{CO}_2^-$  calculated at the MP2/6-311G\* theory level. The CO bond lengths are relaxed (subject to the  $C_{2v}$  symmetry constraint).

presence of neutral  $\text{CO}_2$ . There has been discussion in the literature concerning the relation of this state to the ground state of  $\text{CO}_2^-$  [25–28]. Limiting the present discussion to the  ${}^2A_1$  and  ${}^2B_1$  states arising from the  ${}^2\Pi_u$  resonance, the absorption of 355 nm photons by  $\text{CO}_2^-$  is attributed to the  ${}^2B_1 \leftarrow {}^2A_1$  transition, indicated by a vertical arrow in Fig. 4. It is this transition that the 340 nm absorption band has previously been assigned to [15,17].

The  ${}^2B_1 \leftarrow {}^2A_1$  transition leaves  $\text{CO}_2^-$  with a high degree of bending excitation, with the potential gradient directing the system towards linearity. The  $\text{O}^-({}^2P) + \text{CO}$  dissociation products can be formed on the ground state, suggesting that a portion of the  ${}^2B_1$  excited-state population is funneled to the  ${}^2A_1$  state each time the molecule passes through linearity. Similar Renner–Teller mediated predissociation mechanisms have been implicated in other bent triatomic radicals, with HCO being the classical example [29,30].

Our trajectory calculations indicate that once on the ground electronic state, the dissociation of  $\text{CO}_2^-$  to  $\text{O}^- + \text{CO}$  takes  $\sim 200$  fs. Although these calculations do not account for steric hindrance from the solvent, the time-dependent dynamics implicitly rely on the solvent-induced stabilization preventing the electron from leaving the excited  $\text{CO}_2^-$ . With the initial momentum directed along the  $\text{OCO}^-$  bend, one expects several bending vibrations to occur on the ground-state potential, before the required energy is channeled into the  $\text{O}^- + \text{CO}$  dissociation coordinate.

It is instructive to compare  $\text{CO}_2^-(\text{H}_2\text{O})_m$  to pure  $(\text{CO}_2)_n^-$  cluster anions. Lineberger and co-workers found that UV fragmentation of  $(\text{CO}_2)_n^-$ ,  $n \geq 13$  occurs via the sequential ejection of  $\text{CO}_2$  monomers [31]. Intriguingly, the onset of this channel coincides, approximately, with the reverse core-switching from the monomer-based  $\text{CO}_2^-(\text{CO}_2)_{n-1}$ ,  $7 \leq n \leq 13$  clusters to dimer-based  $(\text{O}_2\text{CCO}_2)^-(\text{CO}_2)_{n-2}$ ,  $n > 13$  [32].  $(\text{CO}_2)_{13}^-$  is believed to be a mix of the monomer and dimer-based structures. The dominant mechanism of  $(\text{CO}_2)_n^-$ ,  $n \geq 13$  dissociation likely involves the dissociation of the order-of-1/2 C–C bond in the covalently bound  $(\text{O}_2\text{CCO}_2)^-$  dimer-anion [33], yielding  $\text{CO}_2^- + \text{CO}_2$  (followed by the evaporation of some solvent  $\text{CO}_2$ ). Hence, even though the dissociation of the anionic core of the cluster does occur, the fragments are not distinguishable from the mere solvent evaporation. For  $(\text{CO}_2)_n^-$ ,  $n < 13$  only a minor  $\text{CO}_3^-$  channel was observed [31,34]. The  $\text{CO}_3^-$  products can be attributed to  $\text{CO}_2^- \rightarrow \text{O}^- + \text{CO}$  dissociation followed by a bimolecular association reaction  $\text{O}^- + \text{CO}_2 \rightarrow \text{CO}_3^-$ . This channel is most relevant for comparison with  $\text{CO}_2^-(\text{H}_2\text{O})_m$ . For  $n \geq 14$ , following the core-switching to dimer-anion based  $(\text{CO}_2)_n^-$  cluster structures, the  $\text{CO}_3^-$  channel is replaced by  $(\text{CO}_2)_m^-$  products.

## 5. Summary

In summary, the fragmentation of  $\text{CO}_2^-(\text{H}_2\text{O})_m$ ,  $m = 3$ –20 cluster anions at 355 nm yields two types of anionic

products:  $\text{O}^-(\text{H}_2\text{O})_{m-k}$  and  $\text{CO}_2^-(\text{H}_2\text{O})_{m-k}$ . The former are proposed to result from excitation of a hydration-stabilized excited state, originating from a low-lying  $\text{CO}_2^-$  resonance, followed by Renner–Teller mediated predissociation of the cluster core. The  $\text{CO}_2^-(\text{H}_2\text{O})_{m-k}$  products evolve by predissociation of the cluster, photodissociation/recombination of  $\text{CO}_2^-$ , and/or a CTTS mechanism.

### Acknowledgement

This work is supported by the NSF grant No. CHE-0134631 and the Packard Fellowship in Science and Engineering.

### References

- [1] C.D. Cooper, R.N. Compton, *Chem. Phys. Lipids* 14 (1972) 29.
- [2] C.D. Cooper, R.N. Compton, *J. Chem. Phys.* 59 (1973) 3550.
- [3] R.N. Compton, P.W. Reinhardt, C.D. Cooper, *J. Chem. Phys.* 63 (1975) 3821.
- [4] I. Shimamura, K. Takahashi (Eds.), *Electron–Molecule Collisions*, Plenum Press, New York, 1984.
- [5] M. Krauss, D. Neumann, *Chem. Phys. Lipids* 14 (1972) 26.
- [6] G.L. Gutsev, R.J. Bartlett, R.N. Compton, *J. Chem. Phys.* 108 (1998) 6756.
- [7] C.E. Klots, *J. Chem. Phys.* 71 (1979) 4172.
- [8] E. Surber, R. Mabbs, T. Habteyes, A. Sanov, *J. Phys. Chem. A* 109 (2005) 4452.
- [9] R. Mabbs, E. Surber, L. Velarde, A. Sanov, *J. Chem. Phys.* 120 (2004) 5148.
- [10] M.A. Johnson, W.C. Lineberger, in: J.M. Farrar, W.H. Saunders (Eds.), *Techniques for the Study of Ion Molecule Reactions*, Wiley, New York, 1988, p. 591.
- [11] E. Surber, S.P. Ananthavel, A. Sanov, *J. Chem. Phys.* 116 (2002) 1920.
- [12] M.L. Alexander, N.E. Levinger, M.A. Johnson, D. Ray, W.C. Lineberger, *J. Chem. Phys.* 88 (1988) 6200.
- [13] A. Sanov, S. Nandi, K.D. Jordan, W.C. Lineberger, *J. Chem. Phys.* 109 (1998) 1264.
- [14] T. Tsukuda, T. Nagata, *J. Phys. Chem. A* 107 (2003) 8476.
- [15] G.W. Chantry, D.H. Whiffen, *Mol. Phys.* 5 (1962) 189.
- [16] J.P. Keene, Y. Raef, A.J. Swallow, in: M. Emert, J.P. Keene, A.J. Swallow (Eds.), *Pulse Radiolysis*, Academic Press, London, New York, 1965, p. 99.
- [17] K.O. Hartman, I.C. Hisatsune, *J. Chem. Phys.* 44 (1966) 1913.
- [18] P.J. Linstrom, W.G. Mallard (Eds.), *NIST Chemistry WebBook, NIST Standard Reference Database No. 69*, National Institute of Standards and Technology, Gaithersburg, MD, 2005.
- [19] G.J. Schulz, *Phys. Rev.* 128 (1962) 178.
- [20] M.J.W. Boness, G.J. Schulz, *Phys. Rev. Lett.* 21 (1968) 1031.
- [21] G.J. Schulz, D. Spence, *Phys. Rev. Lett.* 22 (1969) 47.
- [22] M.A. Huels, L. Parenteau, P. Cloutier, L. Sanche, *J. Chem. Phys.* 103 (1995) 6775.
- [23] T. Sommerfeld, *Phys. Chem. Chem. Phys.* 3 (2001) 2394.
- [24] M.J. Frisch et al., *Gaussian 98, Rev. A.7*, Gaussian, Inc., Pittsburgh, PA, 1998.
- [25] L.A. Morgan, *Phys. Rev. Lett.* 80 (1998) 1873.
- [26] M. Allan, *J. Phys. B* 35 (2002) L387.
- [27] T. Sommerfeld, *J. Phys. B* 36 (2003) L127.
- [28] T. Sommerfeld, H.D. Meyer, L.S. Cederbaum, *Phys. Chem. Chem. Phys.* 6 (2004) 42.
- [29] K. Tanaka, E.R. Davidson, *J. Chem. Phys.* 70 (1979) 2904.
- [30] R.N. Dixon, *Mol. Phys.* 54 (1985) 333.
- [31] M.L. Alexander, M.A. Johnson, N.E. Levinger, W.C. Lineberger, *Phys. Rev. Lett.* 57 (1986) 976.
- [32] T. Tsukuda, M.A. Johnson, T. Nagata, *Chem. Phys. Lett.* 268 (1997) 429.
- [33] S.H. Fleischman, K.D. Jordan, *J. Phys. Chem.* 91 (1987) 1300.
- [34] V. Vorsa, Ph.D. thesis, University of Colorado, 1996.